Title
Comparison of compressed air energy storage process in aquifers and caverns based on the Huntorf CAES plant

Authors
Guo, Chaobin
Pan, Lehua
Zhang, Keni
et al.

Publication Date
2016-11-01

DOI
10.1016/j.apenergy.2016.08.105

Peer reviewed

Comparison and understanding the thermodynamic processes of compressed air energy storage in cavern and aquifer

Chaobin Guo[a], Lehua Pan[b], Curtis M. Oldenburg[b], Keni Zhang[a, b,*], Cai Li[c], Yi Li[d]

a School of Mechanical Engineering, Tongji University, Shanghai 201804, PR China

b Earth and Environmental Sciences Area, Lawrence Berkeley National Laboratory, Berkeley, CA 94720, USA

c China Institute of Geo-Environmental Monitoring, Beijing 100081, PR China

d College of Water Science, Beijing Normal University, Beijing 100875, PR China

Citation for this paper:

Guo, C., Pan, L., Zhang, K., Oldenburg, C.M., Li, C. and Li, Y., 2016. Comparison of compressed air energy storage process in aquifers and caverns based on the Huntorf CAES plant. *Applied energy*, *181*, pp.342-356.

Abstract

An integrated wellbore-reservoir (cavern or aquifer) simulation is carried out based on parameters of Huntorf CAES (compressed air energy storage) plant. Reasonable matches between monitoring data and simulation results are obtained for both in cavern and wellbore. In this study, the hydrodynamic and thermodynamic behaviors of CAES in cavern and aquifer are investigated, such as pressure and temperature distribution and variation in both wellbore and cavern. Performances of CAESA (compressed air energy storage in aquifer) are studied with numerical models and compared with the performances of CAESC (compressed air energy storage in cavern). The comparisons of CAESC and CAESA indicate that the pressure variation in CAESA shows a wider variation range than that in CAESC, while the temperature shows a smooth variation due to the large grain specific heat. The simulation results confirm that the CAES can be achieved in aquifers. Performance of energy storage in aquifer can be similar to or better than CAESC, if the aquifer has appropriate reservoir properties. The impacts of gas bubble volume, formation permeability and aquifer boundary

[*]Corresponding author. 4800 Caoan Road, Jiading District, Shanghai, China. E-mail address: keniz@hotmail.com (Keni Zhang).

permeability are investigated and the results indicate that the increase of gas bubble volume and permeability can improve the efficiency, but the effect is not significant. The gas bubble boundary permeability has slightly effect on the energy efficiency of sustainable daily cycle but can significant affect total sustainable cycle times. The analyze of thermodynamic behaviors in CAESA suggest that more attention should be paid to the heat storage, reservoir properties and two phase flow process.

Keyword: Compressed air energy storage, Huntorf, aquifer, heat storage

Nomenclature

A Wellbore cross-sectional area (m^2)

C_0 Shape factor

g Acceleration of gravity vector(m/s^2)

F Darcy flux vector (kg m^2/s)

H Specific enthalpy (J/kg)

k_1 storage space permeability

k_2 storage space boundary permeability

M Mass or energy accumulation term (kg/m^3, J/m^3)

NK Number of components

NPH Number of phases

P Pressure (Pa)

S saturation

t Time(s)

U Internal energy (J/kg)

z Z-coordinate(m)

β Phase index

ρ Density (kg/m^3)

μ Dynamic viscosity (Pa·s)

u_G, u_L Phase velocity of gas and liquid in the well (m/s)

u_m,u_d velocity of mixture and drift in the well (m/s)

1 Introduction

Large-scale energy storage attracts increasing attention with the rapid development of renewable energy. Among the energy storage options, CAES (compressed air energy storage) is believed to be attractive due to its cost-effective at large temporal scales (from several hours to days) and at a hundreds-of-MW power scale[1].

The thermodynamic behaviors of CAESC (compressed air energy storage in cavern) have been studied in many literatures [2-4]. Kushnir et al.[2] discussed the solutions for air temperature and pressure variations in cavern, which were derived from mass and energy conservation equations. They also conducted sensitivity analyses to identify the dominant parameters that affect the storage temperature and pressure fluctuations. Raju and Khaitan [3] use heat transfer coefficient between the cavern wall and the air to represent the heat loss. A report[4] by Princeton Environmental Institute has summaried the theory, resources, and applications of CAES for wind power.

The injection and production of compressed air involve the use of a wellbore, which was not explicitly included in the system described above. Accurate predictions about temperature and pressure in wellbore and cavern throughout the operating cycle is necessary to understand the thermodynamic behaviors of the cavern and wellbore so as to achieve optimal operational efficiency[5].

The two exiting commercial grid-scale CAES facilities were constructed in rock-salt formations that exist only in specific regions, and that these regions would not always be near an energy source or demand[6]. This leads to the limited employment of large-scale CAES. This geographical limitation can be weakened if aquifers are used as the compressed air storage space, which is analogous to the natural gas storage in aquifers. The feasibility of aquifers for CAES was positively proved through numerical simulations in previous studies, e.g. Oldenburg and Pan [7]and Guo et al. [8]. In addition, field tests had also been reported by Allen[9], proving that the aquifers can be used as the compressed air storage place for CAES. Several projects are under plan or in the design process, such as the CAES plant located at Columbia Hills[10] while there are no real commercial projects of CAESA(Compressed air energy storage in aquifers) that can provide detail information on the thermodynamic behaviors of compressed air flow. The first proposed IEP (Iowa Energy Park) CAESA project has been ceased because of economic reason with a smaller scale than planned[11].

The comparison of CAESC and CAESA can help on understanding the thermodynamic behaviors of CAESA. However, little attention has been devoted to the comparison. Oldenburg and Pan [7] introduced the difference of CAES in cavern and porous media (aquifer) from the theoretical aspects. The energy storage is dominated by variable pressure (pressure gradients) rather than the single pressure value which can be easily evaluated as in a cavern.

An integrated wellbore-reservoir (cavern or aquifer) model is developed and validated based on the parameters of Huntorf CAES plant. The pressure, temperature and energy variations in both wellbore and storage tank (cavern or aquifer) are discussed and compared with an aim to understand the common and different behaviors in thermodynamic. The results can provide helpful information for the design of CAESA projects.

2 Model development

2.1 Model setup

2.1.1 Conceptual model

The conceptual model is developed with the parameters of Huntorf CAES plant, shown in Fig. 1. There are two caverns in Huntorf CAES plant. The NK1 cavern is selected as the research object. The cavern is simplified as a cylinder with a radius of 17.24 m and a height of 150 m, which has a total volume of 140,000 m^3. The model lateral boundary is 10000 m away from injection well, which is distant enough to guarantee the minimum impact of boundary on the system performance.

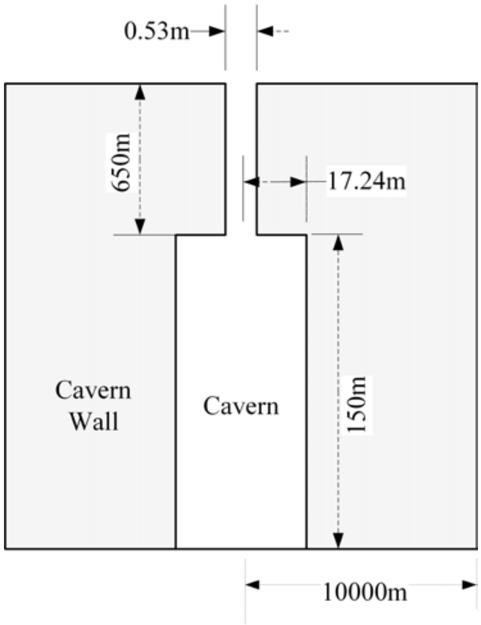

Fig. 1 The conceptual model of CAESC (not to scale)

The major wellbore parameters used in the simulation are shown in Tab. 1.

Tab. 1 Wellbore parameters

Wellbore Parameters	Value	Unit
Diameter	0.553	m
Length	650	m
Roughness	45×10^{-6}	m
Thermal conductivity	2.51	W/m℃

2.1.2 Initial and boundary conditions

The initial conditions are setup with the monitored data of daily cycle. Initially, the cavern is saturated with compressed air and its pressure is 6.0 MPa and temperature is 40 °C. The surrounding formations (cavern wall) are saturated with water. In the vertical direction, they have a geothermal gradient of 31.25 °C/km. There is no fluid flow but heat transfer inside the formations or between the formations and cavern.

The lateral, upper and bottom boundaries are closed with no flow and heat transfer. The injection or production is completed through wellhead.

2.1.3 T2Well/EOS3

The T2Well/EOS3[12] simulator is used to investigate the integrated wellbore-reservoir system., The DFM (drift flux model) approach is used in wellbore and cavern (cavern is also treated as a wellbore) to represent the energy balance, shown in Tab. 2[13]. In reservoir, the mass and energy balance equations are the same as described in TOUGH2[14, 15] and not repeated here.

Tab. 2 Governing equations of wellbore solved in T2well

Parameters	Equation
Momentum equation	$\frac{\partial}{\partial t}(\rho_m u_m)+\frac{1}{A}\frac{\partial}{\partial z}\left[A\sum_{\beta=1}^{NPH}\rho_\beta \mu_\beta^2\right]=-\frac{\partial P}{\partial z}$ $-\frac{\Gamma f \rho_m \lvert u_m \rvert u_m}{2A}-\rho_m g\cos\theta$
Phase velocity	$u_G=C_0\frac{\rho_m}{\rho_m^*}u_m+\frac{\rho_L}{\rho_m^*}u_d$
	$u_L=\frac{(1-S_G C_0)\rho_m}{(1-S_G)\rho_m^*}u_m+\frac{S_G\rho_G}{(1-S_G)\rho_m^*}u_d$
Energy flux	$F^{NK1}=-\lambda\frac{\partial T}{\partial z}+\sum_{\beta=1}^{NPH}\rho_\beta S_\beta \mu_\beta\left(h_\beta+\frac{\mu_\beta^2}{2}+gz\cos\theta\right)$
Energy accumulation	$M^{NK1}=\sum_{\beta=1}^{NPH}\rho_\beta S_\beta(U_\beta+\frac{1}{2}\mu_\beta^2+gz\cos\theta)$

2.2 Model validation with history match

The monitoring data of Huntorf CAES plant were collected from published literatures[5, 16] in order to thoroughly validate the model. Fig. 2 shows the injection and production air flow rates for a typical daily working cycle. The temperature of injection air is 48°C.

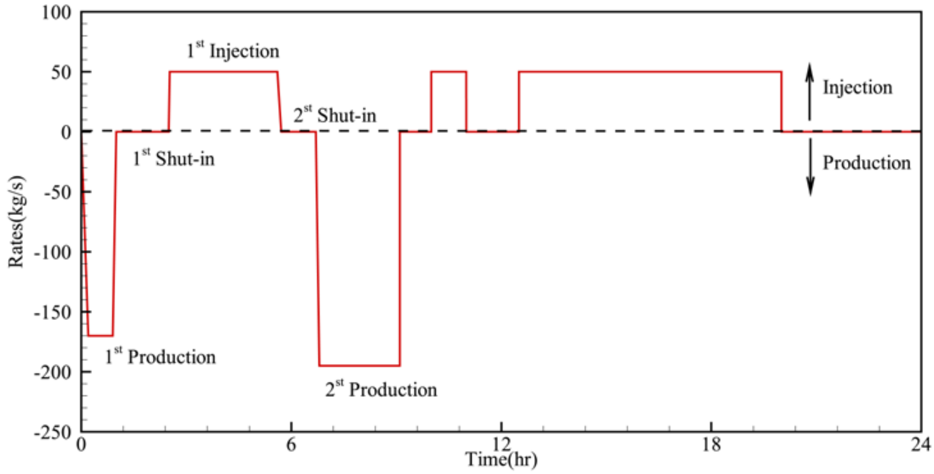

Fig. 2 The injection and production air flow rates collected from literatures

Fig. 3 shows the comparison of monitoring data and simulation results. Good matches between the monitoring data and simulation results are obtained for both cavern and wellbore. Fig. 3a) shows the pressure variation with time together with the flow rate change. The figure shows that the pressure in the cavern and at the wellhead decrease during production period and increase during injection period. Due to compression and expansion, the air temperature increases during injection period and decreases during production period. The modeling results indicate that T2Well/EOS3 module can accurately simulate the thermodynamics behaviors of CAESC. More detail thermodynamics, which cannot be directly observed by monitoring, can be obtained through numerical simulations.

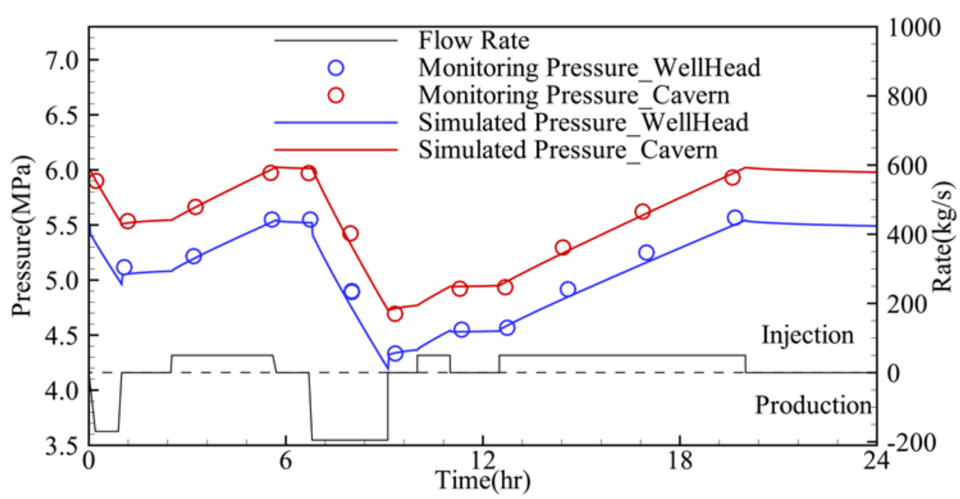

a)

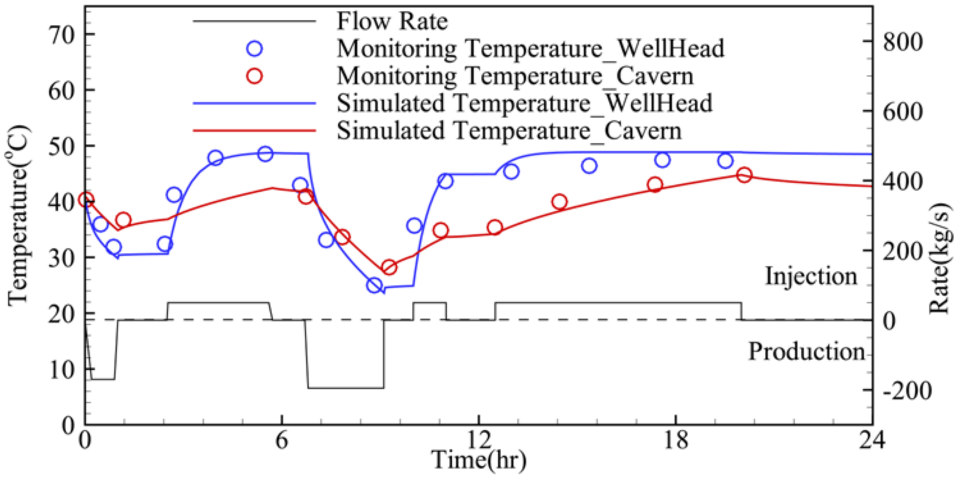

b)

Fig. 3 Pressure, temperature comparison during one operation cycle

3 Thermodynamic behaviors

Further insight into the process modeled can be obtained from Fig. 4, which shows the pressure, temperature and gas density distribution over time in the wellbore and cavern. As shown in Fig. 4(a), at the beginning of operation, the pressure in lower location is slightly larger than it in the upper location because of the gravity. Pressure decreases as the production continue. In the same time, the gas expanding leads to a decrease in temperature, shown in Fig. 4(b).

When it comes to the shut-in period, the pressure at wellhead almost maintains the same level while the pressure of lower location increases slightly. This is because the temperature of cavern is lower than surrounding formations after production, so the cavern gains heat, shown an increase of temperature and pressure. The increase rate of pressure and temperature reduces as temperature difference lessening over time. In addition, the 1^{st} shut-in period is short and the heat transfer does not reach equilibrium.

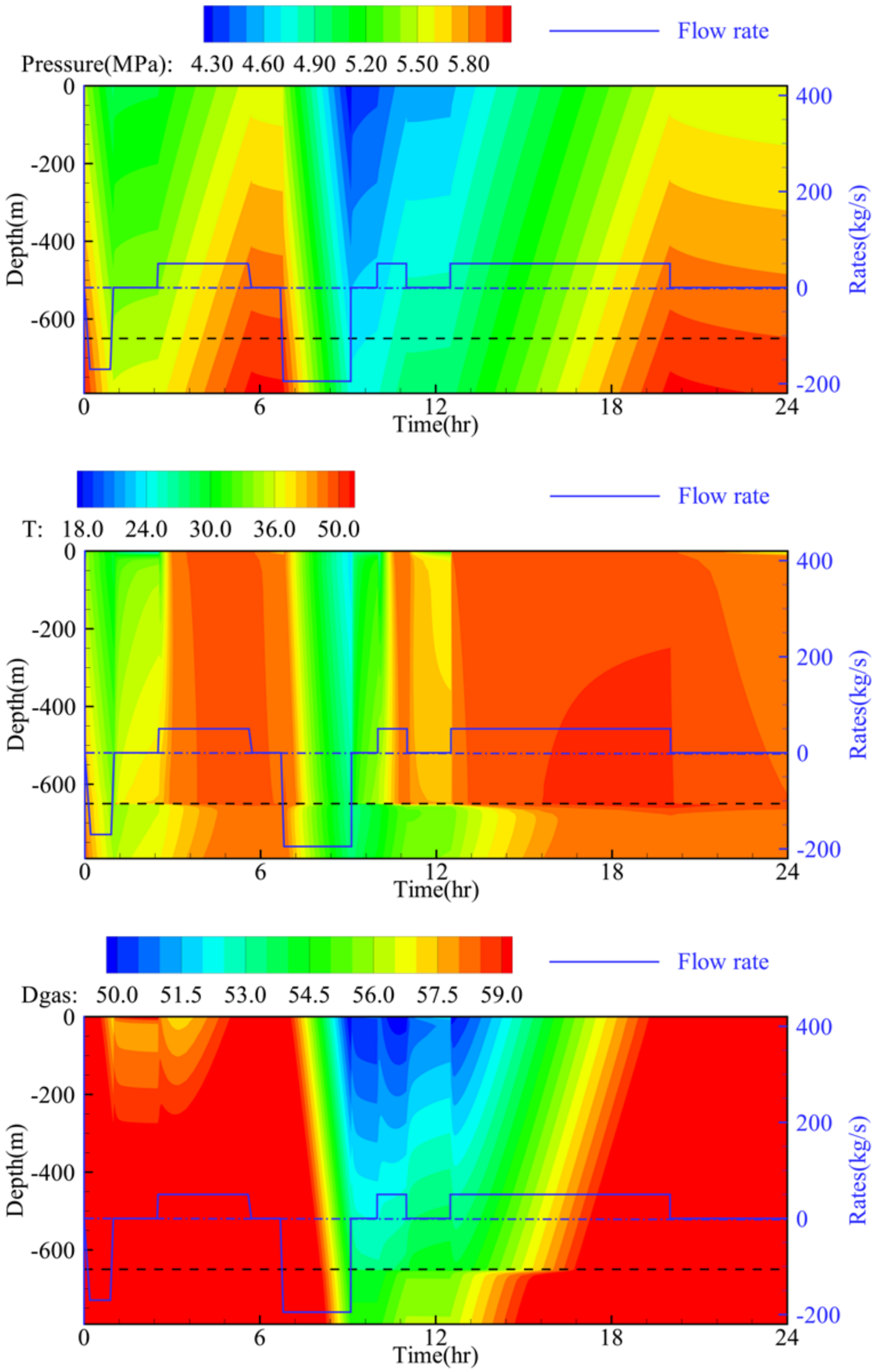

a)

b)

c)

Fig. 4 The pressure, temperature and gas density distribution along the entire length of wellbore and cavern over time in one typical operation cycle

During the injection period, the pressure increases with the increment of air mass. Meanwhile, the temperature increases due to the hot compressed air injection and compression heat caused by the increase of pressure. With the injection continue, a temperature demarcation appears between wellbore and cavern, shown in Fig. 4b). Temperature distribution between wellbore and cavern at three different operation periods is shown in Fig. 5a). With same enthalpy (energy) that flow through and same compression heat (energy) due to pressure increase (Fig. 5b)), the total energy flow rate that go through wellbore and cavern is identical. However, the total energy loss (flow out) through wellbore is less than cavern, which is only about 20% of heat loss through cavern as shown in Fig. 6. This is why the temperature at well bottom is higher than it in the cavern.

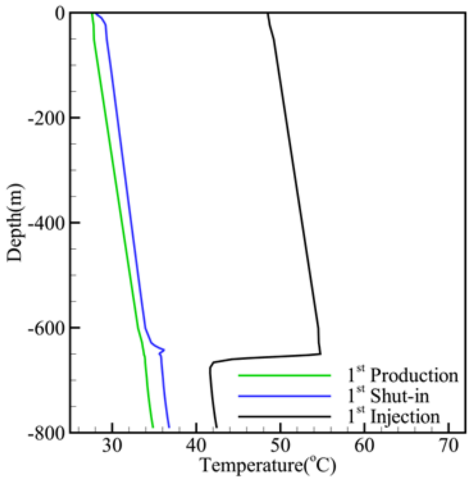

a)

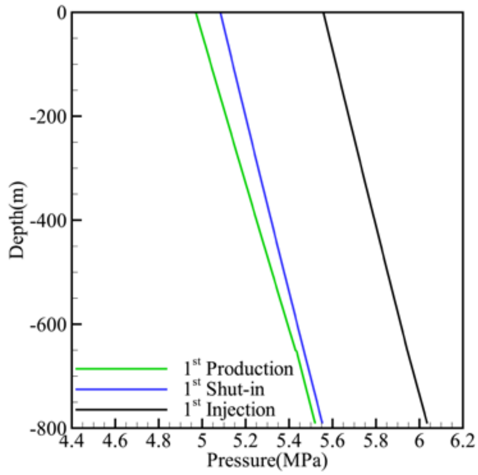

b)

Fig. 5 The pressure and temperature distribution of three different times

Fig. 6 shows the HTR (heat transfer rate) between wellbore-cavern system and surroundings. Positive value means that wellbore or cavern gains heat from surrounding formations. During the production period, wellbore-cavern system gains heat from surrounding formations due to expanding process with pressure decrease. During injection period, wellbore-cavern system loses heat to surrounding formations due to compression heat. The HTR is in the order of a few megawatts and this part of energy should be taken into account for accurate calculations while designing CAES projects. Fig. 7 shows the HTR intensity (kW/m^2) variation, from which we can learn that the heat gains through wellbore is nearly the same as it through cavern during the production period while heat loss through wellbore is larger than it through the cavern during the injection period. This is because the temperature difference along wellbore is larger than it in cavern due to geothermal gradient.

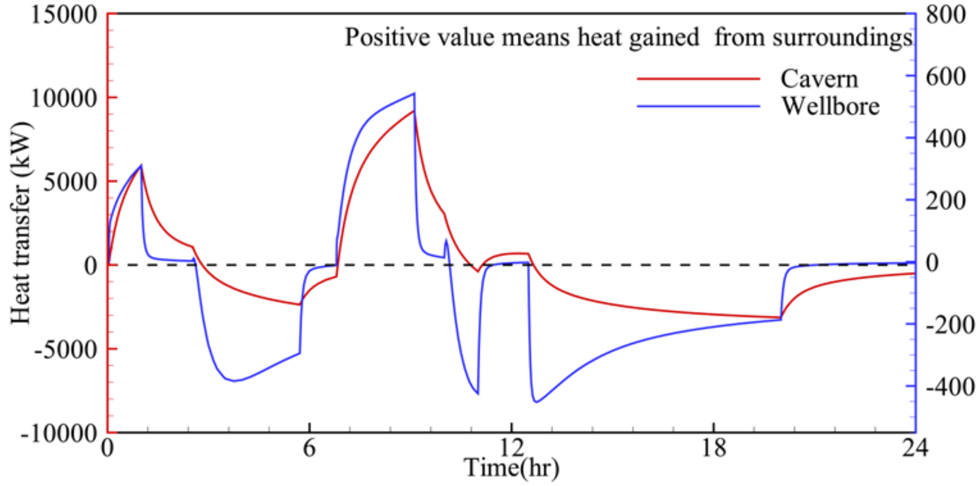

Fig. 6 Comparison of total heat transfer rate between wellbore and cavern

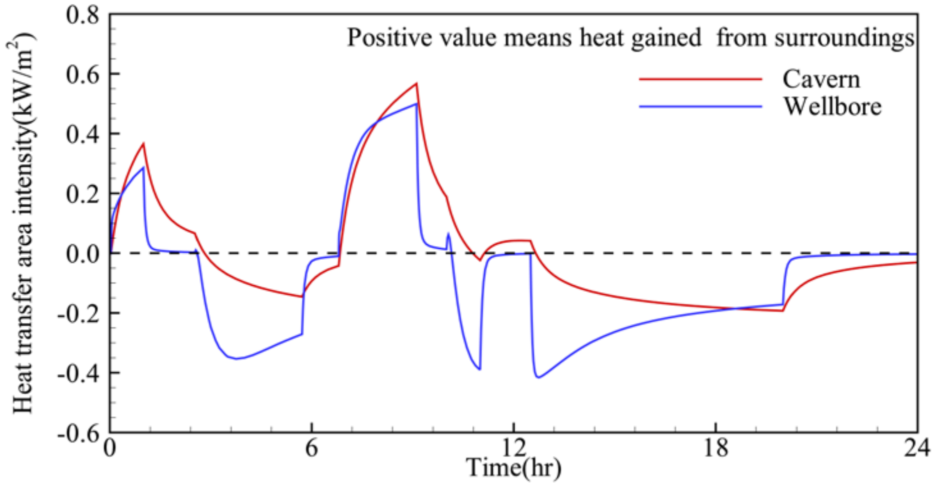

Fig. 7 Comparison of heat transfer rate intensity between wellbore and cavern

At the beginning of 2nd production period, the temperature of both cavern and wellbore is higher than the surrounding formations. This is due to temperature increase during the 1st injection and slightly decrease during short time of 2nd shut-in period. At this moment, both the wellbore and cavern are losing heat to surrounding formations. With production continue, the temperature decreases due to gas expansion, shown in Fig. 8. After production, the temperature difference is about 15 °C in the cavern, which is larger than the temperature difference of surrounding formations (9°C). At this moment the wellbore-cavern is gaining heat from surrounding formations.

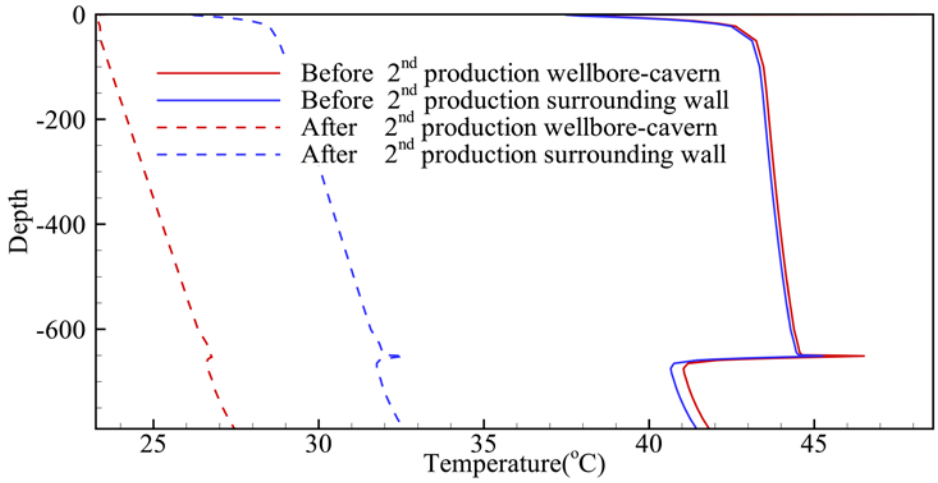

Fig. 8 The temperature distributions of wellbore-cavern and wall before and after the 2nd production period

There is a demarcation between losing heat and gaining heat for the wellbore-cavern system. Fig. 9 Shows the temperature distributions when the total HTR through wellbore or cavern is zero. In Fig. 9a, the red line showing the temperature distribution along the wellbore indicates that the wellhead and the bottom hole have a higher temperature than the surroundings, which will lose heat to the surroundings; while the other parts have a lower temperature, which will gains heat from the surroundings. This makes the total HTR through wellbore to be zero. However, no significant difference in temperature is observed between the cavern and the surroundings when the total HTR is zero, shown in Fig. 9b, because the heat transfer area and the gas volume are large.

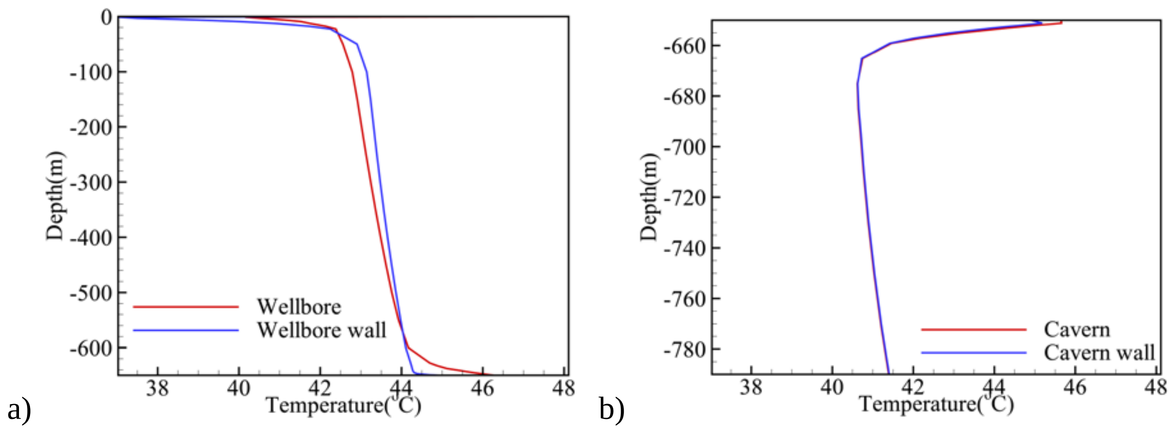

Fig. 9 The temperature distributions for the case of zero total HTR along the: a) wellbore and b) cavern

Fig. 10 shows the energy flow rate during the whole process of one operation cycle. The energy flow rate is 63 MW at largest production rate of 195 kg/s. The ratio of energy flow rate and production mass rate is 0.323 MJ/kg. It is not equal to the energy flow rate of 290MW at 417 kg/s (0.695 MJ/kg) according to Huntorf CAES project. This is because Huntorf's nominal turbine output includes the energy produced by the heating process (added natural gas in the gas turbine).

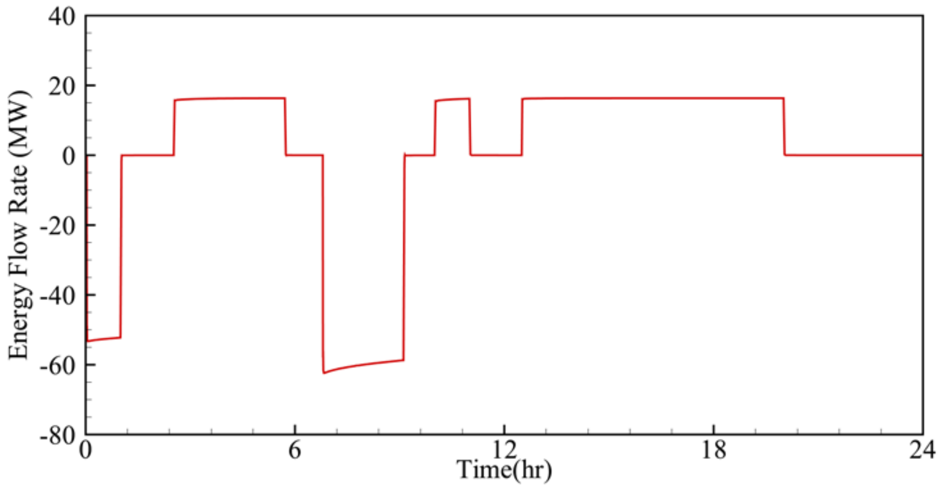

Fig. 10 The energy flow rate in one operation cycle

The developed wellbore-cavern model can be used to characterize the thermodynamic behaviors of compressed air in wellbore and cavern in detail. It would help on understanding the thermodynamic behaviors of the cavern and wellbore so as to achieve optimal operational efficiency.

4 Compressed air energy storage in aquifers

4.1 CAESA model setup

Sandstone is one of the most popular aquifers that are suitable for CAESA. The effective porosity of typical sandstone is 0.05 - 0.30. A report from Princeton University[4] shows that the proper porosity for CAESA should be greater than 0.16.The porosity that used in a related literature of CAESA is 0.2[7]. So we choose 0.2 as the default porosity for this study. The thickness of aquifer is setup with the same thickness as the cavern in Huntorf, which is 150 m. There may exist residual water when the gas bubble is developed in aquifer (initially saturated with water), we choose 0.1 as the residual gas saturation. With the same air volume (140,000 m^3) and porosity of 0.2, the gas bubble radius in aquifer is about 40.63 m.

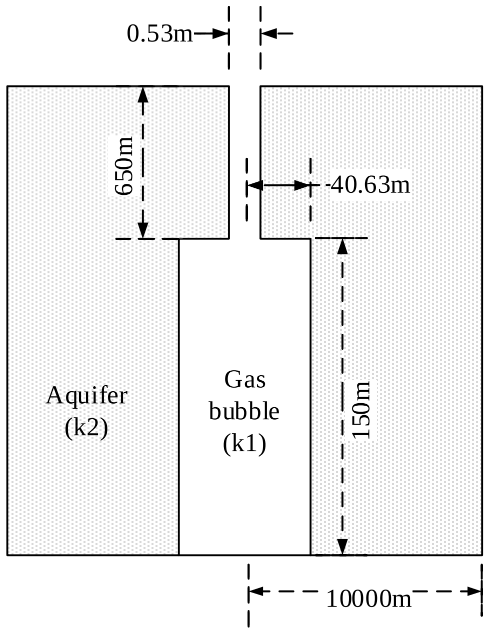

Fig. 11 Conceptual model of CAESA (not to scale)

The aquifer is assumed to be in ideal conditions for CAESA, like being anticline, lenticle or closed fault. The boundary of gas bubble is closed with no fluid flow but with heat transfer. The gas bubble is well developed and initially saturated with compressed air and residual water. This can be achieved in depleted gas fields with closed boundary or by water production with air injection during development of gas bubble. Since there is no real monitoring data about the initial temperature for CAESA, the temperature is considered to be distributed as geothermal gradient of 31.25 °C/km (15 °C at wellhead and 40 °C at well bottom). The boundary of whole model is closed with no flow and heat transfer. The CAESA model is setup with parameters for best equivalent to the CAESC system in order to achieve more reasonable comparison between the two air storage systems.

The same daily operation cycle is applied to CAESA and CAESC model, shown in Fig. 12 [7, 17]. Since we simulate one of the two caverns in Huntorf CAES plant, the injection or production rate is set as half rate of the maximum rate. The injected air mass amount (54 kg/s ×12 hr) is identical to produced air mass (216 kg/s × 3 hr).

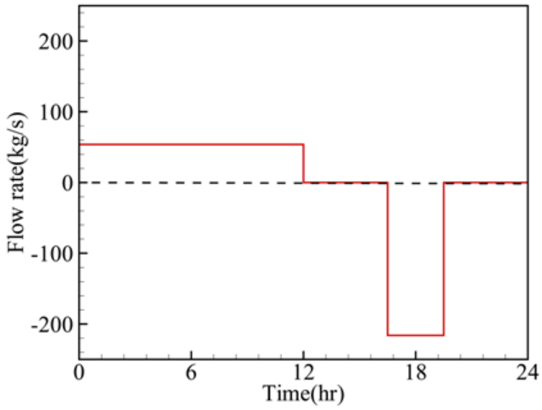

Fig. 12 Injection and production flow rate for operation cycle for both CAESC and CAESA

4.2 Hydrodynamic and thermodynamic behaviors comparison

4.2.1 Pressure and temperature variation

Fig. 13 shows the comparison of wellbore pressure and temperature variation of CAESC and CAESA. The pressure of CAESA shows a wider range than CAESC in both well head and bottom. At the beginning of injection, the pressure in CAESA shows a sudden increase while the pressure reach equilibrium quickly in cavern. This is because the deliverability of gas in porous media (aquifer) is poorer than it in cavern. If the influence of temperature is ignored, the pressure increase rate is the same for CAESC and CAESA after the first sudden increase, shown in Fig. 14. Similarly, the gas cannot migrate quickly from aquifer to wellbore during the production period. Thus, the pressure in aquifer shows a faster drop at the beginning and reaches a lower level than it in cavern after production.

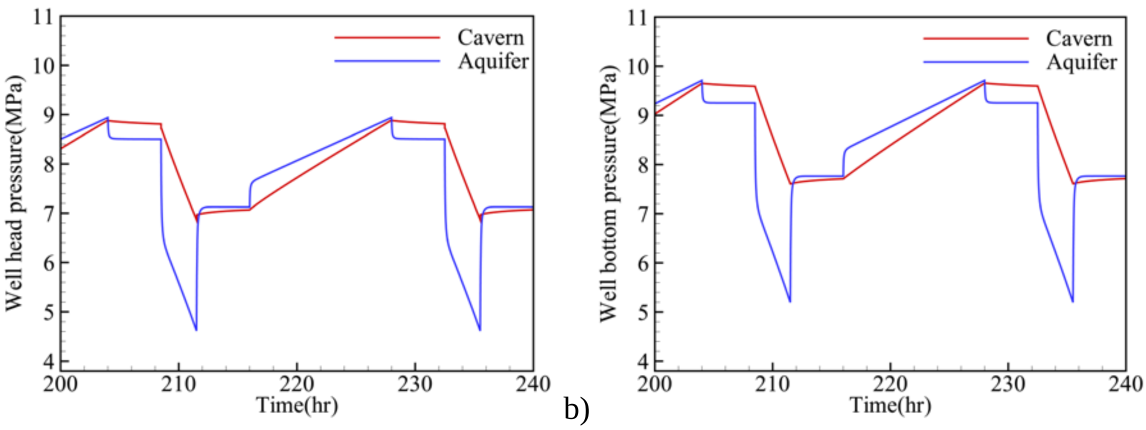

a) b)

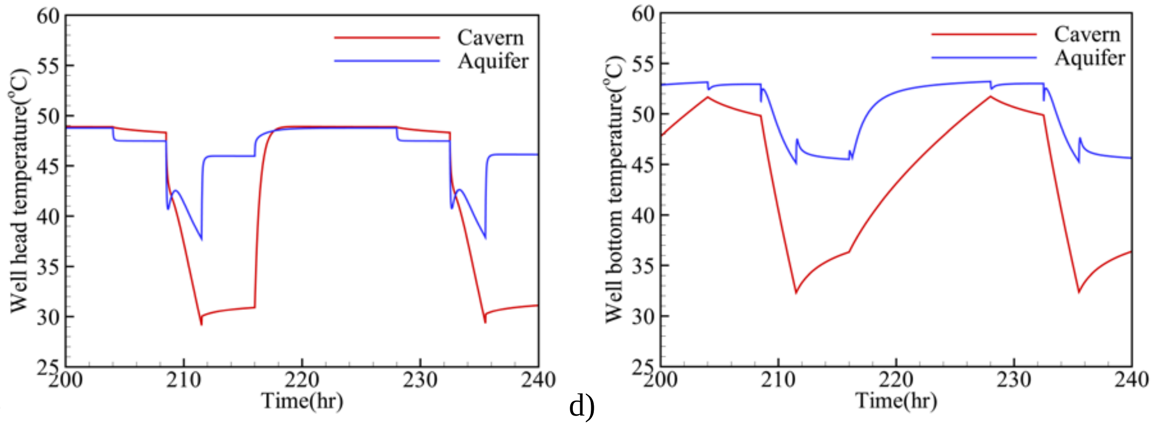

c) d)

Fig. 13 Comparison of the wellbore pressure and temperature variations in CAESC and CAESA

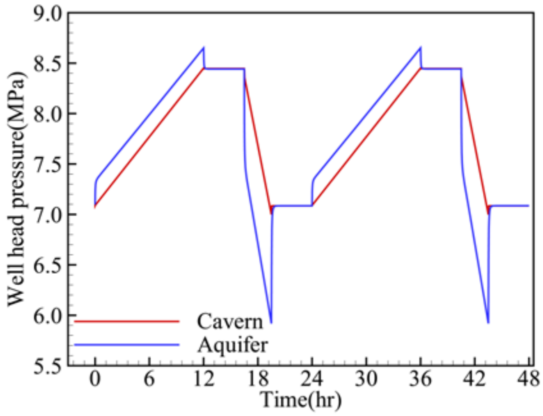

Fig. 14 Pressure variations at wellhead for both CAESC and CAESA under isothermal condition

The temperature of wellbore in CAESA shows smoothly variation than it in cavern because the specific heat of rock grain (920 J/kg °C) is larger than air (720 J/kg °C), shown in Fig. 13(c). With large mass of rock (porosity equals 0.2 and density equals 2600 kg/m^3) and large specific heat, the rock grain in aquifer can hold more energy than air in cavern. Therefore, the temperature varies more gently.

The pressure and temperature distributions over time along wellbore is shown in Fig. 15. The pressure and temperature shows the same trend as it in CAESC. The obvious difference is the pressure and temperature vary abruptly during the alteration of operation. This is because the deliverability of air from aquifer to wellbore is poorer than it in cavern.

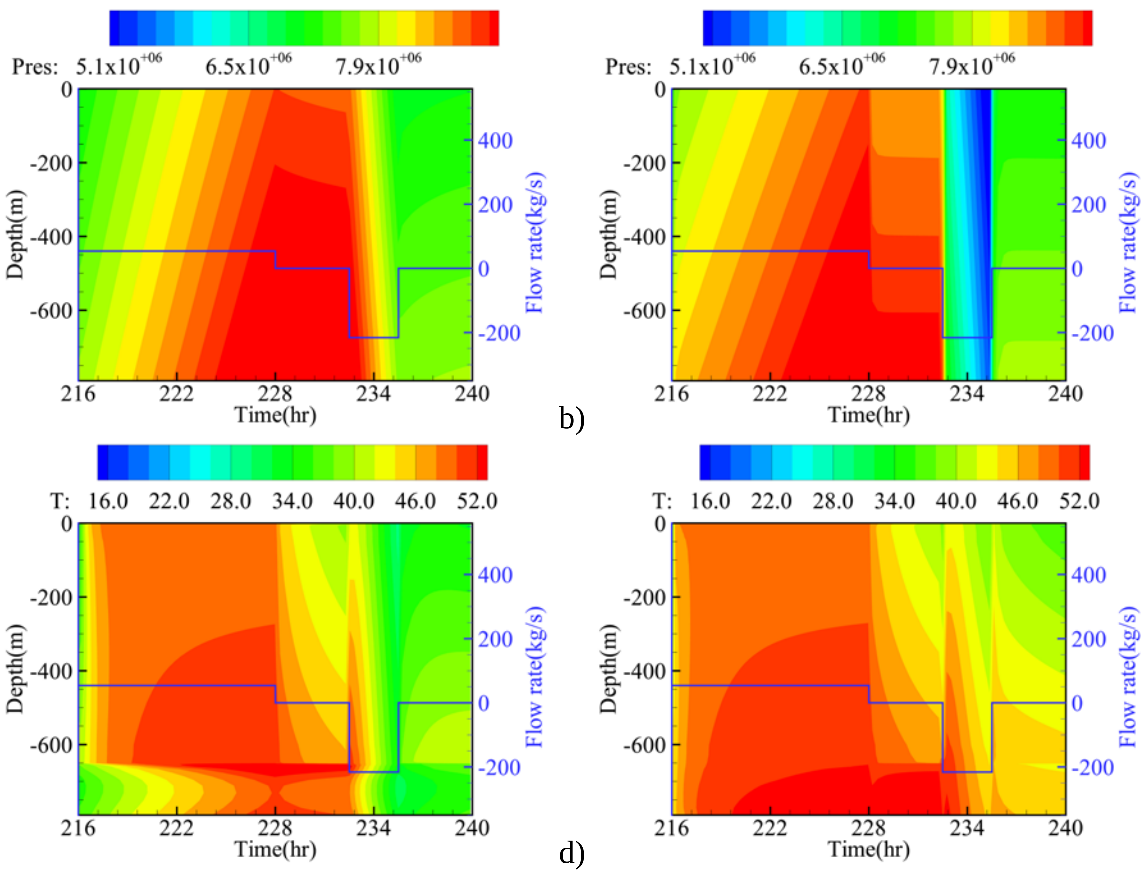

Fig. 15 Pressure and temperature distribution along wellbore over time in an operation cycle for CAESC (a: pressure and c: temperature) and CAESA (b: pressure and d: temperature)

4.2.2 Energy variation

Fig. 16 shows the energy flow rate comparison between CAESC and CAESA. The energy flow rate is almost the same except for the little difference during production period. From the insert figure of Fig. 16, the energy flow rate reduces smoothly in aquifer. This is related to temperature variation. At the beginning of production, the energy flow rate of CAESC is slightly higher than it in CAESA due to the well deliverability of high temperature air in cavern. As the production continue, the air temperature decreases due to gas expanding with pressure decrease. The air in aquifer can get more heat from rock grain, hence it decreases slowly as production continue. We use total injected or produced enthalpy to represent the energy. Thus, a little more (2%) energy can be produced from CAESA (7.52×10^5MJ) than CAESC (7.38×10^5MJ). The total energy injected is 7.62×10^5MJ. The storage efficiency is defined as the ratio of total produced energy to total injected energy.

Therefore, the efficiency of CAESA is about 98.7%, which is higher than the efficiency of CAESC (96.8%). The actual storage efficiency for the Huntorf is about 42%, due to taking efficiency of the facilities at ground surface (compressor and turbine) into account.

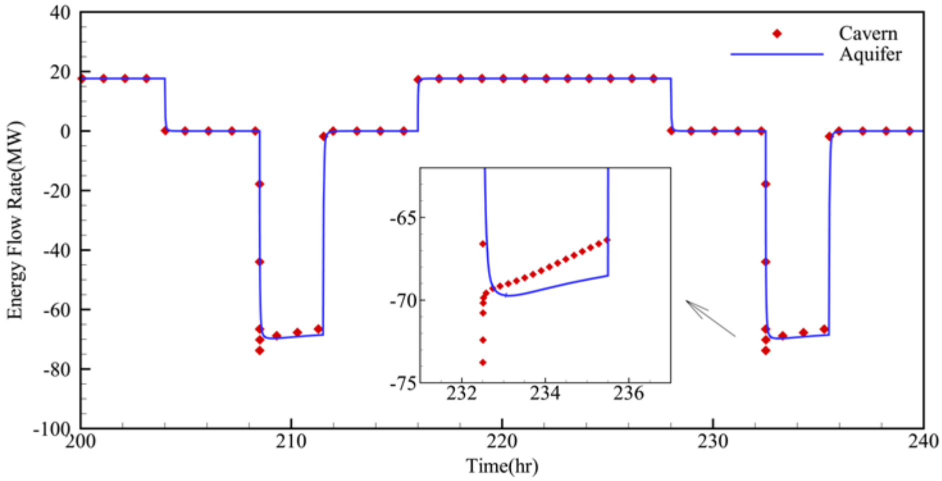

Fig. 16 Comparison of wellbore energy flow rate for CAES in cavern and aquifer

The results of pressure, temperature and energy variation indicate that compressed air energy storage can be achieved in aquifer with appropriate porous media property. One of the differences is the pressure distribution in aquifer is in gradient, unlike the almost single pressure value in cavern. The alteration of operation would cause pressure abruptly variation. This would affect the operational aspects, such as longer system startup time to minimize large pressure variation. In addition, the abruptly change of pressure need high requirements of operation facility.

Another difference is the advantage of rock solid grain heat. The injection air temperature of Huntorf CAES plant is decided by the cavern temperature. For CAESA, the injection air temperature should be optimized based on aquifer rock property, such as specific heat and porosity. Some methods can be applied to make heat be stored in aquifer to improve the storage efficiency.

4.3 Impact of gas bubble volume

One of the important aspects during design CAESA projects is the development of gas bubble. The volume of gas bubble can affect the selection of site and the cost aspect. The gas bubble volume in aforementioned model is 140000 m^3 and it can vary in aquifer depend on reservoir properties. A multiply factor is introduced to represent different gas bubble volume, shown in Tab. 3.

Tab. 3 Different gas bubble volume cases design

Multiplying factor	1.0	5.0	10.0	100.0
Radius (m)	40.63	90.84	128.47	406.26

The pressure and temperature variations under different gas bubble volume are shown in Fig. 17. The pressure increases less with larger volume during injection and decreases to a lower value due to the previous low value during production period. There is little difference for temperature variation during production period. The temperature increases quickly in large gas bubble case during shut-in period due to better deliverability.

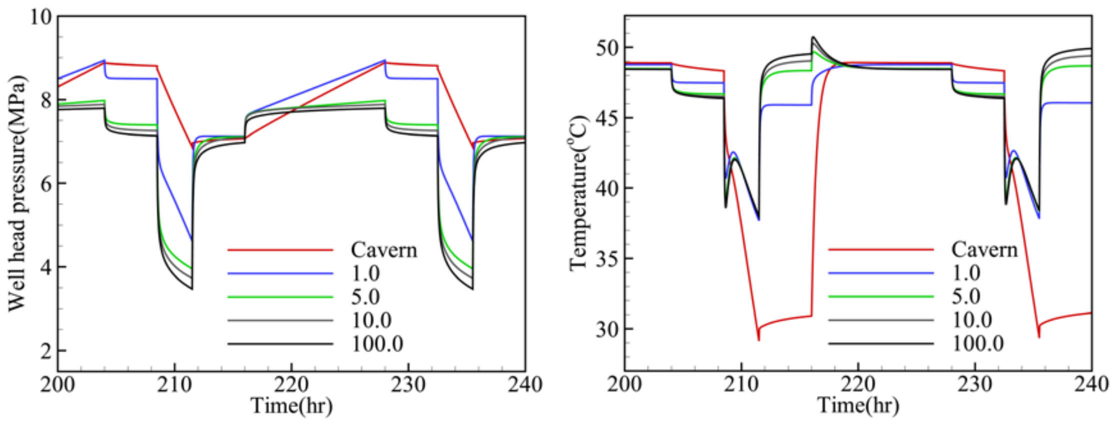

Fig. 17 Pressure and temperature variation for different gas bubble volume cases

Fig. 18 shows the energy flow rate of different gas bubble volume cases during production period of from 208 to 212 hr. The results show that the total energy production increases as gas bubble volume increase. However, the improvement of energy production is only about 0.38% as the gas bubble volume multiplying factor increase from 1.0 to 100.0. And this improvement occurs mainly as multiplying factor increase from 1.0 to 5.0.

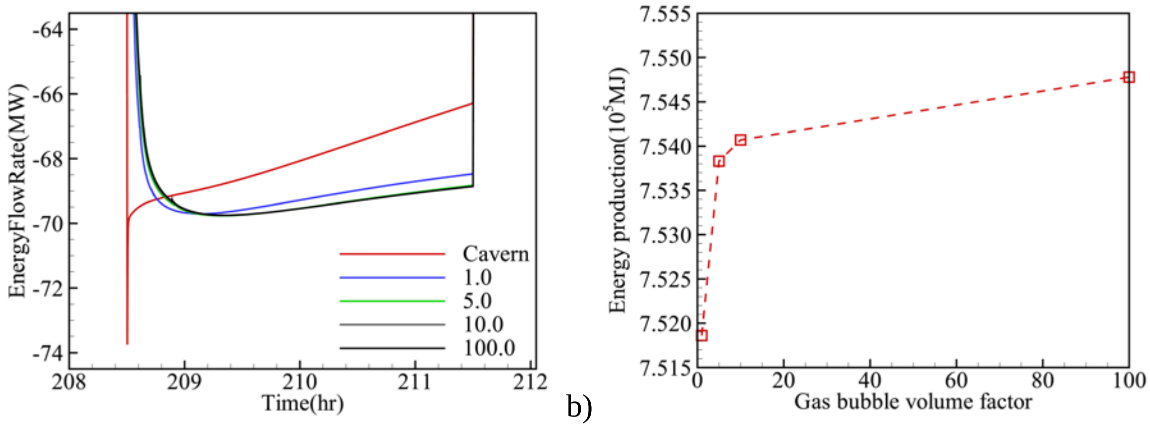

a) b)

Fig. 18 Energy flow rate variation (a) and energy production (b) for different gas bubble volume cases

The increase of gas bubble volume can improve the efficiency but the effect is not significant. We may conclude that it is not necessary to have a very large initial gas bubble.

4.4 Impact of gas bubble formation permeability (k_1)

The formation permeability of gas bubble is another important factor that should be considered during the site selection. In order to investigate the influence of formation permeability, different cases are designed as Tab. 4.

Tab. 4 Case design for different formation permeability

Parameters	Value	Unit
k_2	0.0	m^2
k_1	5.0×10^{-14}	m^2
	1.0×10^{-13}	m^2
	5.0×10^{-13}	m^2
	1.0×10^{-12}	m^2
	1.0×10^{-11}	m^2

The operation cycle cannot be finished under 5.0×10^{-14} m^2. This is mainly because the production rate cannot be achieved due to poor deliverability. The pressure and temperature variation are shown in Fig. 19. As the permeability increases, the pressure variation range decreases and becomes closer to the cavern. The formation permeability has little influence on energy production, except at the beginning of production.

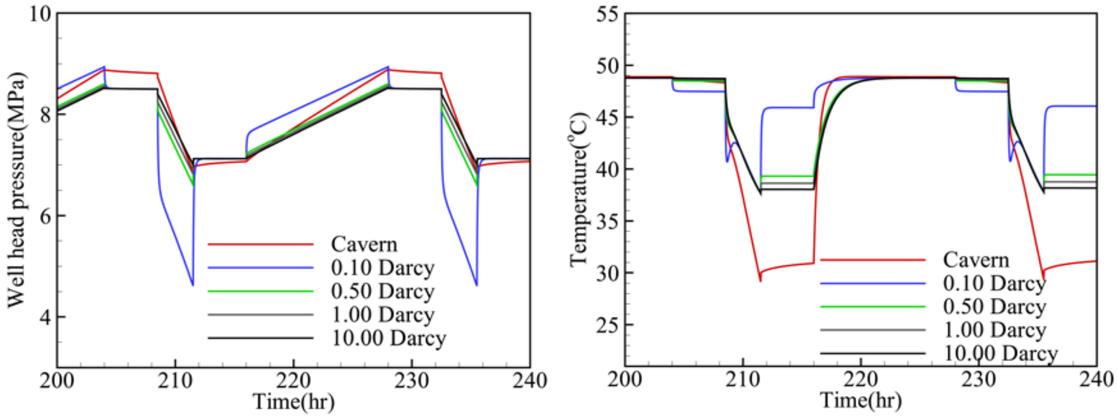

Fig. 19 Pressure and temperature variation for different formation permeability cases (200 hr ~ 240 hr)

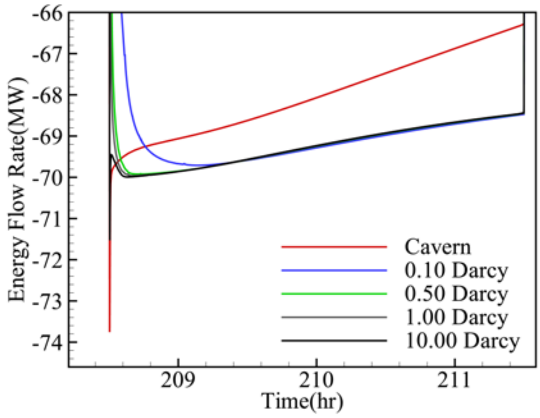

Fig. 20 Energy flow rate for different formation permeability cases (200 hr ~ 240 hr)

The sustainable operation of cycle has a low limit of permeability. Below this value, the certain amount of air cannot be produced. One of the reasons that IOWA project terminated is the energy scale (135 MW) cannot be achieved under low permeability of Dallas Center Mt. Simon[18]. Under low permeability condition, hydraulic fracture or horizontal well can be applied to improve productivity so as to achieve operation cycle. The energy production scale can be up to 65MW when horizontal well is introduced in IOWA project. On the other hand, the increase of permeability can increase the energy scale, but cannot obviously improve daily energy efficiency.

4.5 Impact of gas bubble boundary permeability (k_2)

Unlike cavern with closed cavern walls, the boundary of gas bubble is not completely closed without fluid flow in most common aquifers. That will lead to the difference of thermodynamic behaviors for CAESC and CAESA. Based on the ideal aquifer aforementioned, different permeability cases are designed so as to investigate the influence of boundary permeability for air storage space.

Tab. 5 Cases design of different gas bubble boundary permeability

Parameters	Value	Unit
k_1	1.0×10^{-13}	m^2
k_2	5.0×10^{-13}	m^2
	1.0×10^{-13}	m^2
	1.0×10^{-14}	m^2
	1.0×10^{-15}	m^2
	1.0×10^{-20}	m^2

4.5.1 Pressure and temperature variation

Fig. 21 shows the pressure variations for different boundary permeability conditions. For the comparison between a closed boundary and a low permeability ($1.0\times10^{-20}m^2$), both the maximum pressure (right after injection) and minimum pressure (right after production) remain a relative stable level during the cycles. The maximum pressure with closed boundary is higher than it in lower permeability case due to no flow out of gas bubble. However, the minimum pressure with closed boundary is lower than it in low permeability case. This is because gas bubble can gain pressure support during production due to the large pressure difference even when the permeability is small. As the permeability increase, both the maximum and minimum pressure decrease as cycle continues. The energy loss for the permeable boundary cases is due to pressure gradual propagation to farther away in aquifer during injection, which cannot be recovered during production.

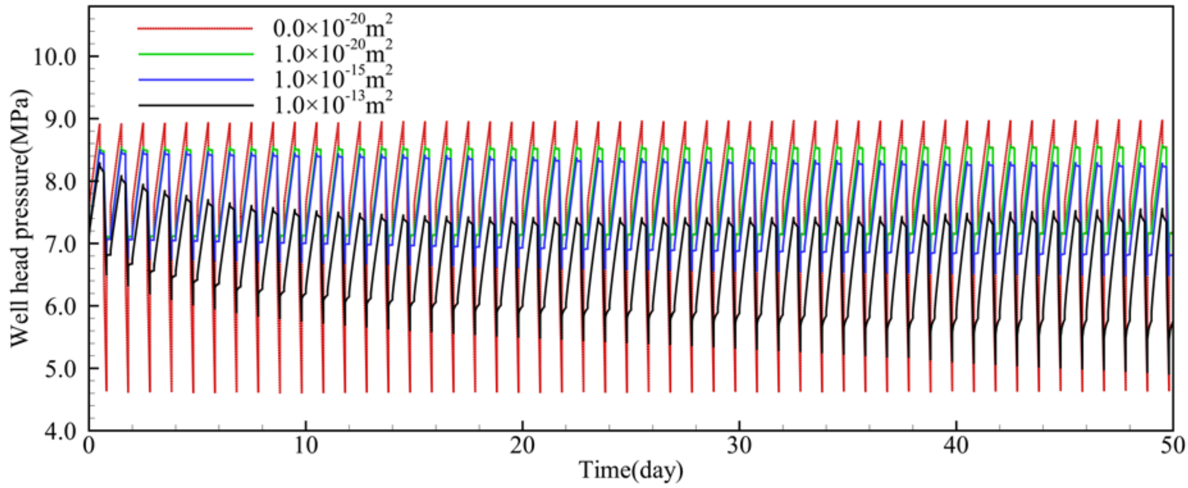

Fig. 21 Pressure variations of different k_2

When k_2 increases to the same as or larger than k_1, the maximum pressure first decrease and then increase with cycle continue, shown in Fig. 22. This is because two-phase flow occurs in wellbore (first occurs at the well bottom), shown in Fig. 23. At 10^{th} day, the saturation of gas bubble area is shown in Fig. 24a), and when it comes to 40^{th} day, water flows into well bottom (Fig. 23 and Fig. 24b)). This is due to the compressed air migrate upward under buoyance and far away under pressure difference during injection.

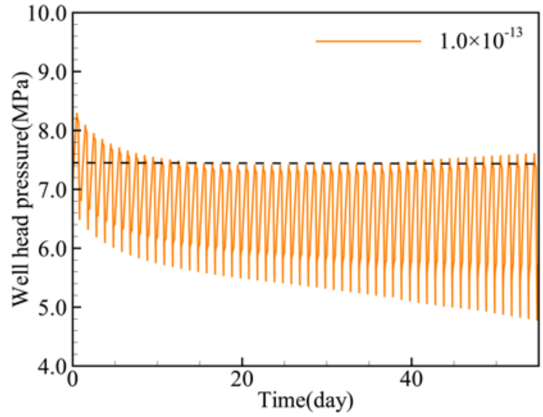

Fig. 22 Pressure variation with gas bubble boundary permeability of 1.00×10^{-13}m^2

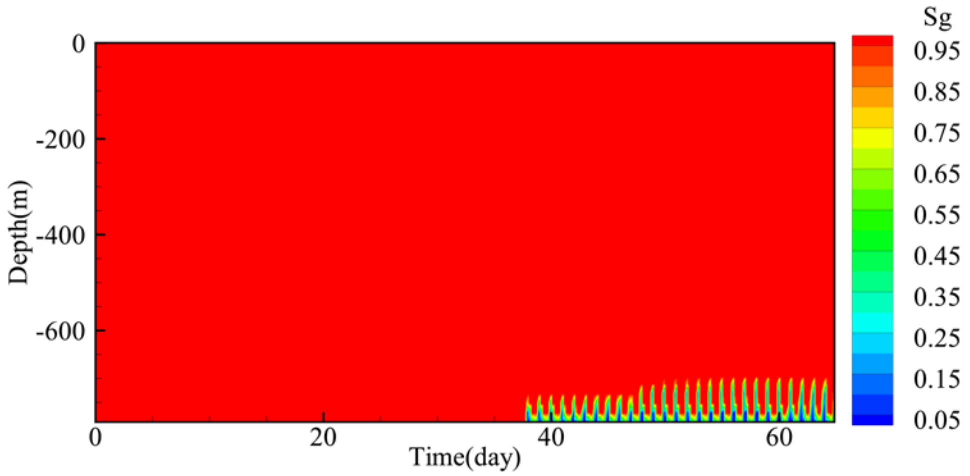

Fig. 23 Gas saturation distribution in wellbore over time for 1.00×10^{-13} model

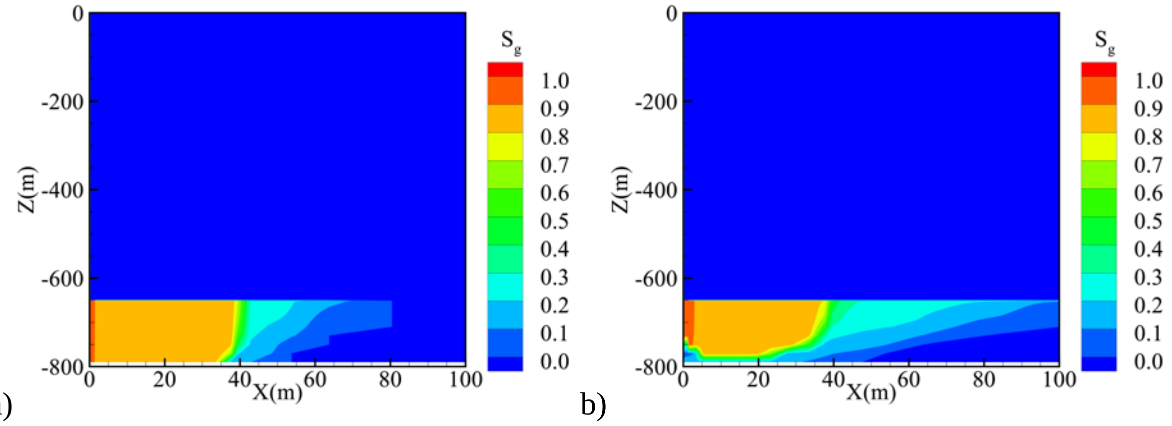

a) b)

Fig. 24 The gas saturation distributions at the a): 10th day and b): 40th day

Fig. 25 shows the temperature variations of different k_2. As cycle continues, the temperature of closed boundary increases a little during injection period. The temperature of injection area gradually increases to the same value (48°C) of injection air temperature as cycle continue. Due to compression heat, the temperature would exceed the injection air temperature during injection period. For all cases, the minimum temperature would increase a little as cycle continue due to injection of hot compressed air. The minimum temperature is lower in larger k_2 due to increase of heat loss.

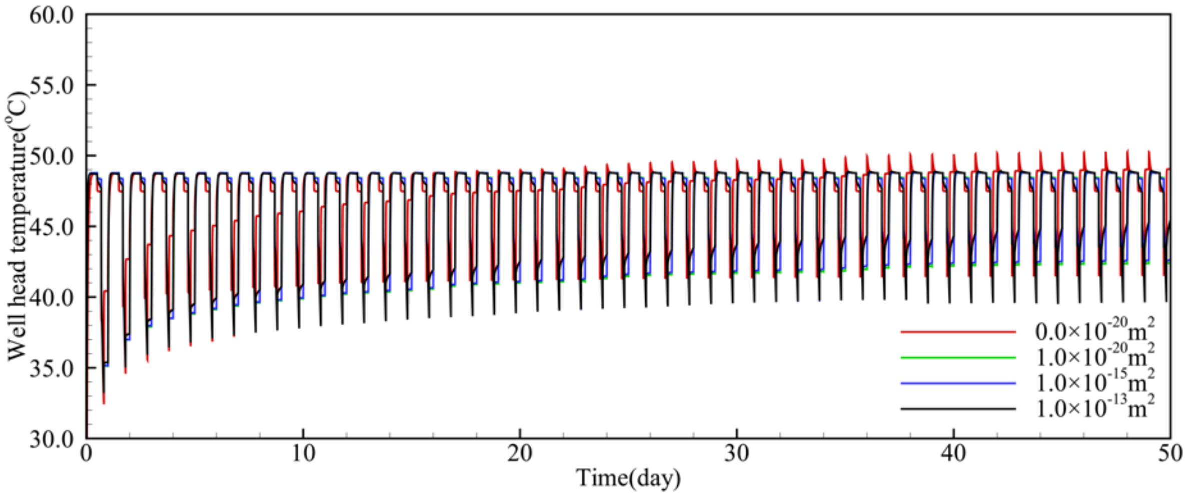

Fig. 25 Temperature variations of different boundary permeability cases

4.5.2 Energy variation

Fig. 26 shows the energy flow rates during production period (49 ~50 day). It is similar to the previous pressure and temperature results. At the beginning of production, the energy flow rate of closed boundary is smaller than the low permeability case. The energy flow rate decreases as k_2 increase and has an sudden decrease when liquid water flows into wellbore when k_2 increases to a certain level, which is 1.0×10^{-13}m^2 in this case.

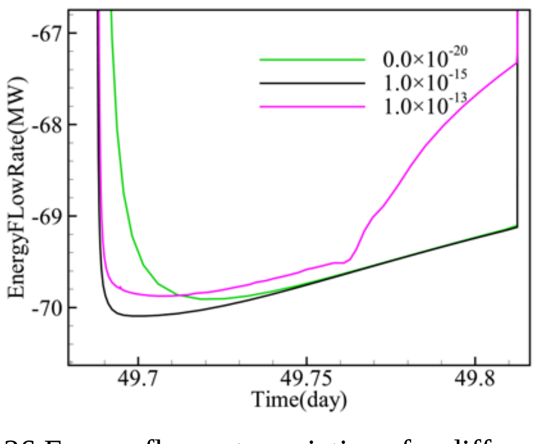

Fig. 26 Energy flow rate variations for different k_2 cases

The gas bubble boundary permeability has slightly effect on the energy efficiency of sustainable daily cycle. This means that the compressed air energy storage can be achieved in horizontal aquifer, and the energy efficiency can be the same or better. However, it can affect the total sustainable cycle times. When a larger amount of water produced, the gas bubble is considered to be unable to support the cycle, leading to system ceased. At this point, certain amount of gas should be injected to make up the gas bubble. The injection of compensation gas can make the cycle continue, while it reduces the total efficiency.

5 Conclusion

Based on the Huntorf CAES plant parameters and monitoring data, we carry out a wellbore-reservoir simulation to investigate and better understand the thermodynamic behaviors of CAES. More detail thermodynamics in both wellbore and cavern, which cannot be directly observed by monitoring, can be obtained through numerical simulations.

The comparison of thermodynamic behaviors between CAESC and CAESA indicate that the CAESA can achieve the same level of energy flow rate for gas storage in appropriate porous media. Operation of injection and production should be appropriately designed due to larger pressure variation for CAESA. The smooth temperature change in aquifers indicates that CAES and geothermal system can be combined to find out proper injection temperature and achieve the best energy efficiency.

CAESA can be influenced by reservoir properties. The increase of gas bubble volume can improve the efficiency but the effect is not obvious, which means it is not necessary to develop a very large gas bubble. Similar conclusion can be drawn for the influence of gas bubble formation permeability. The influence of gas storage space boundary permeability on efficiency of daily cycle is slight. However, the total efficiency drops when the permeability of gas storage space boundary increase to a certain level, which may indicate that some methods should be considered and applied to make up this part of energy loss during designing CAESA projects.

There remain many other aspects for CAESA that should be thoroughgoing studied, such as chemical issues (oxidation issues), safety issues (cap rock and structure integrity). Demonstration projects can be carried out to obtain more detail information about CAESA.

Acknowledgement

This research was granted partly by Fundamental Research Funds for the Central Universities through Beijing Normal University (No.2015KJJCB17). It was also supported by the China Scholarship Council (CSC) for the first author’s visit at Lawrence Berkeley National Laboratory.

Reference

[1] Schainker RB, Rao A. Compressed air energy storage scoping study for california. California,USA: Electric Power Research Institute; 2008.

[2] Kushnir R, Dayan A, Ullmann A. Temperature and pressure variations within compressed air energy storage caverns. International Journal of Heat and Mass Transfer. 2012;55:5616-30.

[3] Raju M, Khaitan SK. Modeling and simulation of compressed air storage in caverns: A case study of the huntorf plant. Applied Energy. 2012;89:474-81.

[4] Succar S, Williams RH. Compressed air energy storage: Theory, resources, and applications for wind power. Princeton environmental institute report. 2008;8.

[5] Crotogino F, Quast P. Compressed-air storage caverns at huntorf. ISRM International Symposium-Rockstore 80: International Society for Rock Mechanics; 1980.

[6] Kim HM. Exploring the concept of compressed air energy storage (caes) in lined rock caverns at shallow depth: A modeling study of air tightness and energy balance. 2012.

[7] Oldenburg CM, Pan L. Porous media compressed-air energy storage (pm-caes): Theory and simulation of the coupled wellbore–reservoir system. Transport in porous media. 2013;97:201-21.

[8] Guo C, Zhang K, Li C. Influence of permeability on the initial gas bubble evolution in compressed air energy storage in aquifers. TOUGH Symposium 2015. Berkeley, California 2015.

[9] Allen RD, Doherty TJ, Kannberg LD. Summary of selected compressed air energy storage studies. Pacific Northwest Labs., Richland, WA (USA); 1985.

[10] Mcgrail B, Cabe J, Davidson C, et al. Technoeconomic performance evaluation of compressed air energy storage in the pacific northwest. Richland: Pacific Northwest National Laboratory; 2013.

[11] Moridis G, King M, Jansen J. Iowa stored energy park compressed-air energy storage project: Compressed-air energy storage candidate site selection evaluation in iowa: Dallas center feasibility analysis. Prepared for the Iowa Stored Energy Plant Agency by The

Hydrodynamics Group. 2007;200:46.

[12] Pan L, Oldenburg CM. T2well—an integrated wellbore–reservoir simulator. Computers & Geosciences. 2014;65:46-55.

[13] Pan L, Freifeld B, Doughty C, et al. Fully coupled wellbore-reservoir modeling of geothermal heat extraction using co2 as the working fluid. Geothermics. 2015;53:100-13.

[14] Pruess K, Oldenburg C, Moridis G. Tough2 user's guide version 2. Lawrence Berkeley National Laboratory. 1999.

[15] Zhang K, Wu Y-S, Pruess K. User’s guide for tough2-mp-a massively parallel version of the tough2 code. Report LBNL-315E, Lawrence Berkeley National Laboratory, Berkeley, CA. 2008.

[16] Crotogino F, Mohmeyer K-U, Scharf R. Huntorf caes: More than 20 years of successful operation. Orlando, Florida, USA. 2001.

[17] Guo C, Zhang K, Li C, et al. Modelling studies for influence factors of gas bubble in compressed air energy storage in aquifers. Energy. 2016;107:48-59.

[18] Schulte RH, Critelli Jr N, Holst K, et al. Lessons from iowa: Development of a 270 megawatt compressed air energy storage project in midwest independent system operator. Sandia National Laboratories, Albuquerque. 2012.